

**AIR-DRILL WITH ACCELEROMETER AND
MICROPHONE FOR COMPOSITE DRILLING
APPLICATION**

By:

KOH WEI TONG

(Matrix No.: 142795)

Supervisor:

Dr. Mohd Syakirin Bin Rusdi

15th July 2022

This dissertation is submitted to
Universiti Sains Malaysia
As partial fulfilment of the requirement to graduate with honors degree in
BACHELOR OF ENGINEERING (MECHANICAL ENGINEERING)



**School of Mechanical Engineering
Engineering Campus
Universiti Sains Malaysia**

DECLARATION

This work has not previously been accepted in substance for any degree and is not being concurrently submitted in candidature for any degree.

Signed..... (KOH WEI TONG)

Date.....

Statement 1: This journal is the result of my own investigation, except where otherwise stated. Other sources are acknowledged by giving explicit references.

Bibliography/ references are appended.

Signed..... (KOH WEI TONG)

Date.....

Statement 2: I hereby give consent for my journal, if accepted, to be available for photocopying and for interlibrary loan, and for the title and summary to be made available outside organizations.

Signed..... (KOH WEI TONG)

Date.....

ACKNOWLEDGEMENT

The completion of this project and thesis was the result of the combined effort of not just me but also many people. First of all, I would like to express my utmost gratitude to Dr. Mohd Syakirin Bin Rusdi for his guidance throughout this project and also providing me with his access to the apparatus and materials needed for this experiment such as the air drill, drill bits and Solidworks model of jig from Spirit AeroSystems Malaysia Sdn Bhd. Besides, Dr Syakirin Rusdi have constantly provide a lot of crucial advice, guidance and knowledges for me to progress on this works.

Next, I would also like to sincerely thank Dr. Muhammad Hafiz Bin Hassan for providing key materials for the experiment such as CFRP plates and GFRP plates. Other than that, Dr Hafiz have also provided help to cut the large CFRP plates and GFRP plates to smaller sizes to be fitted within the 3D printed jig.

Moreover, Dr. Muhammad Fauzinizam Bin Razali also deserve to have my gratitude for providing 3D printing services multiple times to print the self-designed jig. He has also provided many tips during designing of the jig to make fabrication of it possible.

My sincere thanks to research officer and assistance engineers from School of Mechanical Engineering especially Mr. Wan Mohd Amri Wan Mamat Ali who have providing me technical assistance to collect the experimental data. The accelerometer, microphone and LMS SCADAS Mobile used in the experiment was setup and operate by Mr. Wan Mohd Amri Wan Mamat Ali during the experiment.

Lastly, I am grateful with my parents and my friends for their financial and emotional support throughout my undergraduate study throughout this project.

TABLE OF CONTENT

| | |
|---|-------------|
| DECLARATION..... | ii |
| ACKNOWLEDGEMENT..... | iii |
| TABLE OF CONTENT..... | iv |
| LIST OF TABLES..... | vi |
| LIST OF FIGURES..... | viii |
| LIST OF ABBREVIATIONS..... | x |
| ABSTRAK..... | xi |
| ABSTRACT..... | xii |
| CHAPTER 1 INTRODUCTION..... | 1 |
| 1.1 Carbon Fibre Reinforced Polymer (CFRP)..... | 1 |
| 1.2 Glass Fibre Reinforced Polymer (GFRP)..... | 1 |
| 1.3 Drilling of Composite..... | 2 |
| 1.4 Tool Condition Monitoring systems (TCMs)..... | 3 |
| 1.5 Problem Statement..... | 3 |
| 1.6 Objective..... | 3 |
| 1.7 Scope of Work..... | 4 |
| CHAPTER 2 LITERATURE REVIEW..... | 5 |
| 2.1 Vibration as Methods in Tool Condition Monitoring Systems..... | 5 |
| 2.2 Sounds as Methods in Tool Monitoring Systems..... | 9 |
| CHAPTER 3 RESEARCH METHODOLOGY..... | 11 |
| 3.1 Fabrication of Jig..... | 11 |
| 3.2 Preparation of CFRP Plates and GFRP Plates..... | 12 |
| 3.3 Specification of LMS SCADAS Mobile, Accelerometer and Microphone..... | 13 |
| 3.4 Setup of LMS SCADAS Mobile, Accelerometer and Microphone..... | 16 |
| 3.5 Preparation of Drill Bits..... | 17 |

| | | |
|--|---|-----------|
| 3.6 | Conduction of the Experiment | 17 |
| CHAPTER 4 RESULT AND DISCUSSION..... | | 19 |
| 4.1 | Amplitude versus Time Graph | 19 |
| 4.2 | FFT Graph | 27 |
| 4.3 | Images Captured using Alicona SFM | 43 |
| CHAPTER 5 CONCLUSION AND FUTURE WORKS | | 49 |
| 5.1 | Conclusion..... | 49 |
| 5.2 | Future Works | 50 |
| REFERENCE | | 52 |
| APPENDIX | | 58 |

LIST OF TABLES

| | |
|---|----|
| Table 3-1: Codes assigned for each hole | 18 |
| Table 4-1: FFT graph obtained from vibration measured by accelerometer, C1 during drilling of CFRP plate. | 33 |
| Table 4-2: FFT graph obtained from vibration measured by accelerometer, C1 during drilling of GFRP plate. | 34 |
| Table 4-3: FFT graph obtained from vibration measured by accelerometer, C2 during drilling of CFRP plate. | 35 |
| Table 4-4: FFT graph obtained from vibration measured by accelerometer, C2 during drilling of GFRP plate. | 36 |
| Table 4-5: FFT graph obtained from vibration measured by accelerometer, C4 during drilling of CFRP plate. | 37 |
| Table 4-6: FFT graph obtained from vibration measured by accelerometer, C4 during drilling of GFRP plate. | 38 |
| Table 4-7: FFT graph obtained from sound measured by microphone, C3 during drilling of CFRP plate. | 39 |
| Table 4-8: FFT graph obtained from sound measured by microphone, C3 during drilling of GFRP plate. | 40 |
| Table 4-9: Observation and comparison of significant peaks frequencies from FFT graph for drilling of CFRP plate | 41 |
| Table 4-10: Observation and comparison of significant peaks frequencies from FFT graph for drilling of GFRP plate | 42 |
| Table 4-11: Images of front side of drilled holes on CFRP plate taken using Alicona SFM. | 45 |
| Table 4-12: Images of back side of drilled holes on CFRP plate taken using Alicona SFM. | 46 |
| Table 4-13: Images of front side of drilled holes on GFRP plate taken using Alicona SFM. | 47 |
| Table 4-14: Images of back side of drilled holes on GFRP plate taken using Alicona SFM. | 48 |
| Table 5-1: Vibration amplitude measured by accelerometer, C1 versus time graph obtained during drilling of CFRP plate. | 61 |

| | |
|--|----|
| Table 5-2:Vibration amplitude measured by accelerometer, C1 versus time graph obtained during drilling of GFRP plate. | 62 |
| Table 5-3: Vibration amplitude measured by accelerometer, C2 versus time graph obtained during drilling of CFRP plate..... | 63 |
| Table 5-4: Vibration amplitude measured by accelerometer, C2 versus time graph obtained during drilling of GFRP plate. | 64 |
| Table 5-5: Vibration amplitude measured by accelerometer, C4 versus time graph obtained during drilling of CFRP plate..... | 65 |
| Table 5-6: Vibration amplitude measured by accelerometer, C4 versus time graph obtained during drilling of GFRP plate. | 66 |
| Table 5-7: Sound amplitude measured by microphone, C3 versus time graph obtained during drilling of CFRP plate. | 67 |
| Table 5-8: Sound amplitude measured by microphone, C3 versus time graph obtained during drilling of GFRP plate. | 68 |

LIST OF FIGURES

| | |
|--|----|
| Figure 3-1: 3D model of jig used in industry for drilling of composite material | 11 |
| Figure 3-2: Closer look on features available on jig..... | 11 |
| Figure 3-3: 3D printed jig | 12 |
| Figure 3-4: The CFRP plates (left) and the GFRP plates (right) with size of about 9cm×18.5cm..... | 13 |
| Figure 3-5: LMS SCADAS Mobile | 13 |
| Figure 3-6: Accelerometer | 14 |
| Figure 3-7: Specifications of accelerometer | 15 |
| Figure 3-8: BSWA microphone | 15 |
| Figure 3-9: Full specification of the microphones | 16 |
| Figure 3-10: Positions of accelerometer C1, C2 and C4 on air drills | 16 |
| Figure 3-11: Schematic Diagrams of the experiment setups. | 17 |
| Figure 3-12: The posture and handling of the air drill during drilling of composite plate..... | 18 |
| Figure 4-1: Maximum amplitude of air drill vibration measured by accelerometer C1 during drilling of CFRP plate versus condition of drill bit..... | 20 |
| Figure 4-2: Maximum amplitude of air drill vibration measured by accelerometer C1 during drilling of GFRP plate versus condition of drill bit..... | 21 |
| Figure 4-3: Maximum amplitude of air drill vibration measured by accelerometer C2 during drilling of CFRP plate versus condition of drill bit..... | 22 |
| Figure 4-4: Maximum amplitude of air drill vibration measured by accelerometer C2 during drilling of GFRP plate versus condition of drill bit..... | 22 |
| Figure 4-5: Maximum amplitude of air drill vibration measured by accelerometer C4 during drilling of CFRP plate versus condition of drill bit..... | 23 |
| Figure 4-6: Maximum amplitude of air drill vibration measured by accelerometer C4 during drilling of GFRP plate versus condition of drill bit..... | 24 |
| Figure 4-7: Maximum amplitude of air drill vibration measured by accelerometer C3 during drilling of CFRP plate versus condition of drill bit..... | 25 |
| Figure 4-8: Maximum amplitude of air drill vibration measured by accelerometer C3 during drilling of GFRP plate versus condition of drill bit..... | 25 |
| Figure 5-1: 3D model of jig used for fixture of composite plate during drilling process in Spirit AeroSystems Sdn Bhd. | 58 |

| | |
|--|----|
| Figure 5-2: Drawing of jig designed for this experiment..... | 59 |
| Figure 5-3:The whole setup of the experiment in SME laboratory | 60 |
| Figure 5-4: Images of drill bits of different conditions..... | 60 |

LIST OF ABBREVIATIONS

| | |
|-------|---|
| AE | Acoustic Emission |
| ANFIS | Adaptive Network-based Fuzzy Inference System |
| ANN | Artificial Neural Network |
| AOE | Acousto-optic emissions |
| CFRP | Carbon fibre reinforced polymer |
| CNC | Computer Numerical Control |
| CWT | Continuous Wavelet Transform |
| DCAE | Deep Convolutional Autoencoder |
| EMD | Empirical Mode Decomposition |
| FFT | Fast Fourier Transforms |
| FRPs | Fibre Reinforced Polymers |
| GFRP | Glass fibre reinforced polymer |
| ICA | Independent Component Analysis |
| IMFs | Intrinsic Mode Functions |
| LDV | Laser Doppler vibrometer |
| PCA | Principal Components Analysis |
| PSD | Power Spectrum Density |
| RMS | Root Mean Square |
| SFs | Signal Features |
| SVMs | Support Vector Machines |
| TCM | Tool Condition Monitoring |
| TCMs | Tool Condition Monitoring Systems |
| VB | Flank Wear |

GERUDI PNEUMATIK DENGAN ACCELEROMETER AND MIKROFON UNTUK APLIKASI PENGGERUDIAN KOMPOSIT

ABSTRAK

Kejejasan ketepatan dimensi dan toleransi penggabungan akibat kehausan bit gerudi boleh menyebabkan masalah serius seperti perpecahan bahagian struktur kapal terbang dalam jumlah yang besar. Untuk memastikan lubang tbuk dalam bahan komposit mempunyai kualiti yang baik dari pelbagai aspek, prosedur yang diamalkan dalam industri adalah pelupusan bit gerudi yang jumlah lubang yang ditebuknya sebanyak bilangan ditetapkan. Namun begitu, amalan ini boleh menyebabkan pembaziran sesetengah bit gerudi yang masih boleh menebuk lubang yang tidak adanya delaminasi walaupun jumlah lubang yang ditebuk menggunakan bit gerudi tersebut sudah melebihi bilangan yang ditetapkan. Untuk memantau kondisi alat mesin, para penyelidik telah melakukan pelbagai eksperimen untuk menghubungkan kehausan bit gerudi dengan pembolehkan proses seperti daya pemotongan, daya tujahan, getaran dan pelepasan akustik. Penyelidikan ini mengemukakan sebuah sistem pemantauan alatan yang menggunakan getaran gerudi angin dan maximum bunyi yang dihasilkan semasa penggerudian bahan komposit. Dalam penyelidikan ini, kesan ketajaman bit gerudi terhadap getaran gerudi pneumatik, bunyi yang dihasilkan semasa penggerudian dan kualiti lubang yang dihasilkan akan diselidikan. Dalam experiment ini, accelerometer dilekatkan pada 3 lokasi berbeza di permukaan drill pneumatik untuk mengukur daya getarannya. Mikrofon diletakkan di tempat yang berjarak 1 meter dari jig untuk mengukur bunyi yang dihasilkan semasa penggerudian komposit. Getaran drill peumatik dan bunyi yang dihasilkan semasa penggerudian menggunakan drill bit yang berbeza kondisinya telah dianalisis dan dibandingkan. Hasil eksperimen menunjukkan getaran yang diukur oleh accelerometer yang paling dekat dengan spindle gerudi adalah paling sensitif dengan kondisi bit gerudi yang berbeza. Untuk, plat CFRP, amplitud getaran gerudi pneumatik maksimum meningkat dengan kondisi drill pneumatic dalam susunan: tajam, tidak ada bit gerudi, haus, dan cip off. Untuk, plat GFRP, amplitud getaran gerudi pneumatik maksimum meningkat dengan kondisi drill pneumatic dalam susunan: tidak ada bit gerudi, haus, cip off, dan bit tajam. Selain itu, alihragam Fourier Cepat signal getaran yang diukur oleh accelerometer ini menunjukkan terdapatnya set frekuensi unik dengan kondisi drill bit yang berbeza.

AIR-DRILL WITH ACCELEROMETER AND MICROPHONE FOR COMPOSITE DRILLING APPLICATION

ABSTRACT

Impaired dimensional accuracy and assembly tolerance due to tool wear could lead to serious problems such as part rejections in substantial amounts on the structure of aircraft. To make sure that drilled holes in composite materials are of good quality from various aspects, current practice in the industries was the disposal of the drill bits after it is being used for a predetermined number of cycles. However, this leads to wastage of some of the expensive drill bits which can still produce holes without delamination even though it has been used for a predetermined number of cycles. To monitor the tools condition, researchers have conducted various experiments to correlate tool wear with process variables such as cutting force, thrust force, vibrations, spindle current, acoustic emission etc. In this research, the effect of sharpness of drill bits on vibrations of air drill, sound produced during drilling and quality of holes produced will be studied. In this experiment, 3 accelerometers have been attached on locations near the spindle, at the middle and near the handle of air drill to measure the vibrations of the air drill. Microphone was placed about 1 meter away from the jig and the sounds produced during drilling process were collected. The vibrations of air drill and sound produced during drilling with different conditions of drill bit are analysed and compared. The result shows that vibrations measured by accelerometer placed nearest to the spindle are most sensitive to change in condition of drill bit. For CFRP plate, maximum amplitude of air drill vibration increases with condition of air drill in order: sharp, no drill bit, blunt, and chipped off. For GFRP plate, maximum amplitude of air drill vibration increases with condition of air drill in order: no drill bit, blunt, chipped off and sharp. Other than that, the fast Fourier Transform of the vibration signals from this accelerometer shows that there was a unique set of frequencies with significant peaks with different conditions of drill bits.

CHAPTER 1

INTRODUCTION

1.1 Carbon Fibre Reinforced Polymer (CFRP)

Composite materials are frequently employed in the aerospace industry, allowing engineers to overcome challenges that would have been encountered if the elements were used separately. The identities of constituent materials in the composites remain and do not dissolve or otherwise blend into one another. The components combine to form a 'hybrid' material with increased structural qualities. Among various type of the composites materials fibre-reinforced polymers (FRPs) are the most often utilised composite materials in manufacturing of aircraft. Their distinct characteristics, such as excellent performance, reduced weight, increased stiffness, and improved corrosion resistance, make them an appealing option for aviation applications(Teti, 2002). The reinforcing fibres in FRPs are typically rigid, stiff, and widely scattered throughout the composite phases imbedded inside the matrix(Callister, 2007). Because the weight may be transmitted to other nearby fibres through the matrix if a single fibre breaks, the reinforcement is also the principal loadbearing element(CallisterJr, 2007). Carbon fibre reinforced plastic (CFRP) was one of the most common fibre-reinforced plastics in the aerospace sector, and it will be the subject of our research. CFRP is commonly employed in aircraft wing boxes, horizontal and vertical stabilisers, and wing panels due to its remarkable strength-to-weight ratio(Soutis, 2005).

1.2 Glass Fibre Reinforced Polymer (GFRP)

Other than CFRP, another type of fibre reinforced polymers commonly used in manufacturing and aerospace industry was the glass fibre reinforced polymer (GFRP) which is also the subject of study in this final year project. Indoors, rubber sealing, landing gears, fuselage body, tail spoiler, and body are examples of GFRP uses in aircraft, which result in weight reductions of 20 to 30 percent compared to metal parts(Shivanagere, Sharma, & Goyal, 2018). In the matrix of GFRP, organic, polyester, thermostable, vinylester, phenolic, and epoxy resins were used. Bisphenolic, ortho, and isophthalic are the two types of the polyester resins(López et al., 2012). The desired physical and functional features of GFRP composites were equivalent to steel,

had better stiffness than aluminium, and had a specific gravity of one-quarter that of steel, attributed to appropriate fibre compositions and orientation(Awan, Ali, Ghauri, Ramzan, & Ehsan, 2009).

1.3 Drilling of Composite

In the assembly stage of aeroplane structural parts, a high number of holes are required to produce riveted and bolted connections(Che, Saxena, Han, Guo, & Ehmann, 2014). Subsequently, drilling become the principal operation for making bolted or riveted assemblies in CFRP components or structures used in industry(Abrão, Rubio, Faria, & Davim, 2008). In a small single-engine plane, more than 100,000 holes are drilled for fasteners like rivets, bolts, and nuts, while in a huge transport plane, millions of holes are drilled(El-Sonbaty, Khashaba, & Machaly, 2004). During drilling of CFPR, delamination induced by drilling become main challenge in the industry and it is a major failure mechanism of composite materials(Wisnom, 2012). In simple terms, delamination is a kind of composite material failure in which the material cracks into layers. Damage produced by delamination development causes in a reduction in strength, toughness, and fatigue life(Khan, Kim, & Kim, 2019). Besides, delamination impairs the dimensional accuracy and surface smoothness of machined holes, resulting in 60 percent of all component rejection at the assembly stage(Giasin, Ayvar-Soberanis, & Hodzic, 2015). Impairment on dimensional accuracy and assembly tolerance could leads to serious problem such as part dismissals in substantial amount(Latha, Senthilkumar, & Palanikumar, 2011). Furthermore, present of delamination on the subsurface on the structure of aircraft can be remain undetected for long period and could leads to unexpected catastrophic failure which may end with countless casualties(Taylor, 2008).

Based on industrial experience, worn drill leads to more delamination on the drilled holes and researchers have found this to be true. The experimental results show that, while the critical thrust force increases with wear, delamination becomes more likely because the real thrust force increases with wear to a greater extent. When compared to a sharp drill, the worn twist drill allows for a reduced feed rate, which prevents delamination damage(Tsao & Hocheng, 2007). Other than delamination, drill wear is a critical problem during the drilling process of conventional or composite materials, resulting in changes in the properties of the created holes as well as cutting tool failure(K.S. Lokesh , Thomas Pinto, 2017).

1.4 Tool Condition Monitoring systems (TCMs)

In the attempt to monitor or predicts the wearing of drill bits, researchers have conduct various experiment to correlate tool wear with process variables such as cutting force(Cuš & Župerl, 2011; Patra, Jha, Szalay, Ranjan, & Monostori, 2017), thrust force(Fernández-Pérez, Cantero, Díaz-Álvarez, & Miguélez, 2019), vibrations(Harun, Ghazali, & Yusoff, 2017; Prasad & Reddy, 2019; Uekita & Takaya, 2017b) and acoustic emission(Uekita & Takaya, 2017a; Vununu, Moon, Lee, & Kwon, 2018). Combined use of machine vision and deep learning method have also been applied for development of TCMs (Atli, Urhan, Ertürk, & Sönmez, 2006). Despite the present of many researches on monitoring of tool wear which involved the use of expensive sensor and equipment, the concise research on the effect of tool wears on acoustics emission and thrust force during drilling of carbon fibre reinforced plastic. Therefore, the objective of our research is to investigate the correlation between vibration, sound and tool wear during conventional drilling of CFRP using tungsten carbide drill bits.

1.5 Problem Statement

To prevent the occurrence of delamination or fibre pull-out on drilled hole due to dull drill bits, industries currently practicing the disposal of drill bits after a predetermined number of cycles of usage on their air drill for composite materials drilling. However, the used drill bits were probably to be still sharp enough to drill more holes without delamination even though is have been use for predetermined number of cycles before. Therefore, the objective of this study is to determine the condition of drill bits based on the sound and vibration produced during drilling of composite.

1.6 Objective

- To investigate the correlation between conditions of tungsten carbide drill bits and vibrations of air drill during conventional drilling of carbon fibre reinforced plastic and glass fibre reinforced plastic using pneumatic drills.
- To investigate the correlation between conditions of tungsten carbide drill bits and sound produced during conventional drilling of carbon fibre reinforced plastic and glass fibre reinforced plastic using pneumatic drills.

1.7 Scope of Work

In this research, the experimental study on the between sound, vibration and tool wear produced during drilling of composite materials is to be done. Thus, parameters that need to be studied are limited to sound, vibration and tool wear of drill bits. The method of drilling will be conventional drilling using customized air drill obtained from aerospace industry while the drill bits used is made of tungsten carbide. The composite materials which will be drilled is carbon fibre reinforced plastic (CFRP) and glass fibre reinforced plastic (GFRP)

CHAPTER 2

LITERATURE REVIEW

Currently, there are many studies was conducted to correlate tool wear with vibrations produced during drilling or milling of composite materials, these studies is contributed greatly to the effort of developing more effective, new tool condition monitoring methods.

2.1 Vibration as Methods in Tool Condition Monitoring Systems

Prasad & Reddy, 2019 conduct research on detecting drilling tool vibrations throughout the drilling operation. In the methodology, the vibration is measured using a laser Doppler vibrometer (LDV), which is a non-contact vibration transducer. Cutting forces and vibration signal features (SFs) are recorded and analysed as cutting tool wear progresses in dry machining of Ti-6Al-4V and Al7075. In conclusion, the vibration parameter displacement and cutting force values followed a similar pattern as the drill bit's tool wear progressed throughout the experiment. To have better understanding on tool life under vibratory cutting scenarios, this research proposes a modified mathematical model. In the current study, determining the link between tool wear, cutting forces, and vibration displacement is a key job. These findings are utilised to predict how displacement and tool wear will change over time in the experiment.

Vununu et al., 2018 present a machine fault diagnosis system that is based on sound generate during drilling. The proposed drill-specific machine fault diagnosis system not only capable to identify faulty drills but also to determine whether the noises were made during the active or idle stages of the entire machinery system, allowing for total remote control. In the process of identifying the faulty drills, the sound's power spectrum is represented as images, and various modifications are applied to them in order to unveil, expose, and highlight the underlying health patterns. The resulting images, known as power spectrum density (PSD) images, are then fed into a deep convolutional autoencoder (DCAE) for feature extraction at a high level. The scheme's last stage is using the suggested PSD-images + DCAE features as the final representation of the original sounds as inputs to a nonlinear classifier, the outputs of which will constitute the final diagnostic decision. The result of this work

shows that the suggested PSD-images + DCAE characteristics have a good discrimination capacity for making a final diagnostic decision. They were also evaluated on a noisy dataset, with the results demonstrating their noise resistance.

Harun et al., 2017 investigate tool condition monitoring using tri-axial acceleration and force sensors in this work instead of the single-axis sensor employed by other researchers. Cutting factors such as cutting speeds, feeds, and depth of cut were examined in deep twist drills. Three-axis data from vibrations and force sensors were used to quantify the impacts on tool condition during cutting operations, which were then examined in the time and frequency domain. In terms of sensor comparison, the paper revealed that both signals showed identical occurrences in terms of vibrations and force, as well as the ability to detect tool drill failure criterion. Vibrations are more appropriate than force for assessing tool condition, according to a case study of deep drilling.

Uekita & Takaya, 2017b present a tool condition monitoring technique for deep-hole drilling that will ensure the quality of precision large-scale components and an energy-based chatter criterion that can be applied throughout long-term manufacturing. In more detail, a new approach combines short-time Fourier transform and spectral kurtosis analysis in the time–frequency domain to detect significant chatter and transient vibration information from an accelerometer signal. Despite the fact that the balance between chatter and dampening effect is extremely delicate, the result shows that the suggested system is capable of warning machine tools prior to failure by continuously monitoring an energy-based chatter criteria throughout long-term manufacturing operation. Not only is the suggested approach effective in preventing tool failure by detecting the onset of chatter, but it also offers detailed information on the tool's status.

Uekita & Takaya, 2017a also have proposed an unique tool condition monitoring (TCM) system based on a multi-sensor fusion technique that combines spindle motor current, AE, and adaptive thresholding for many manufacturing processes. Tool lifetime tests utilising a test piece are carried out at each phase to study the tool deterioration process. AE signals are discovered to offer full tool state information on tool flank wear, fracture propagation, and severe adhesive wear via qualitative assessment. Provisional alert levels are established in the TCM system

using a two-dimensional diagram with regard to both sensors after careful evaluation of such properties. Based on the result, the suggested TCM system not only has a high ability to prevent catastrophic tool failure and surface imperfections in form milling, but it also has a reasonable expendability for varied groove specifications.

Vikram, Ratnam, & Narayana, 2016 investigate the effect of machining parameters on Surface Roughness (Ra) and Tool Vibrations (VIB) in manufacturing operational methods like tangential and orthogonal turn-milling processes. In this experiment, the Laser Doppler Vibrometer (LDV) is used to capture online Acousto-optic emissions (AOE) of tool shank vibrations, which are then evaluated using the VibSoft analyzer. Fast Fourier Transforms (FFT) over time domain data are utilised to identify peak vibration displacements of the cutting tool shanks, which are used for vibration diagnostics and prognostics as a measure of machine tool condition monitoring. In conclusion, due to the laser beam in tangential turn-milling is perpendicular to the shearing action of the rotating tool and rotating workpiece, the number of peaks in frequency spectra seems to be large, simulating the impact of other components inclusion. In orthogonal turn-milling, the laser beams are directed in the direction of the shearing action of the rotary tool and rotating workpiece, resulting in a single high peak frequency spectrum approximating the tool displacement, with the other components' impacts being low in peaks.

X. Zhang, Zhang, Zhang, Li, & Zhao, 2018 proposes a non-contact cutter runout calibration approach that may be easily adapted to apply to other spindle speeds. A numerical optimization approach for finding cutter runout parameters is described based on the recorded relative fluctuation of teeth using the eddy current sensor measurement system. The method's main benefit is that it is straightforward and convenient to use, especially when analysing cutter runout at various spindle speeds. The study results show that the cutter runout has a spindle speed dependent characteristics, which is due to the change of vibration response of spindle system under different spindle speeds.

Jauregui et al., 2018 proposed a method for assessing tool wear by taking simultaneous force and vibration measurements and evaluating them using frequency and time-frequency approaches. The tool wear estimation is obtained by analysing the FFT and Continuous Wavelet Transform (CWT) simultaneously, as well as the

fluctuations in frequency, amplitude, and the existence of nonlinear responses as the cutting progresses. A robust and precise tool wear evaluation is achieved using a combination of force and vibration data, as well as FFT and CWT approaches. Harmonic and nonharmonic frequencies are found in the nominal values of a healthy tool. These harmonic components either differed from the nominal values or were non-existent in the event of a worn tool. Additionally, as the tool wears, the vibration signal analysis reveals the presence of additional frequencies.

Caggiano, Angelone, Napolitano, Nele, & Teti, 2018 aim to monitor the sensors of tool conditions in drilling of stacks comprised of two carbon fibre reinforced plastic (CFRP) laminates. For this purpose, a machine learning method based on acquisition and processing of thrust force, torque, acoustic emission, and vibration sensor signals during drilling is proposed. Supervised feature selection method to cut off unnecessary features followed by an unsupervised feature extraction method based on Principal Components Analysis (PCA) was developed to minimise the sensory features' enormous dimensionality. Result from the machine learning shows a very accurate diagnosis of tool wear (flank wear in term of VB) was achieved, with ANN predicted values very near to the measured tool wear values and root mean squared error at 2.17E-03.

Aralikatti, Ravikumar, Kumar, Shivananda Nayaka, & Sugumaran, 2020 investigate tool condition monitoring using cutting force signals in conjunction with machine learning techniques. In this paper, the results of tool defect classification utilising both vibration and cutting force signals are compared, as well as the machine learning technique. Discrete wavelet features were obtained from the collected vibration and cutting force signals using discrete wavelet transformation. For each signal, the modification gave eight features. The J48 decision tree algorithm was used to select significant features that provide meaningful information about different types of tool condition. To classify the tool's defective condition, the Nave Bayes method was utilised. To train the algorithm, tenfold cross validation was performed. The algorithm was trained using 66% of the entire data and tested with the remaining 34%. The cutting force signal was categorised with 96.667 percent accuracy by the Nave Bayes algorithm, whereas the vibration signal was classified with 70 percent accuracy.

Zhou, Guo, & Sun, 2021 established an integrated wireless vibration detecting tool holder and extracting the singularity aspects of vibration signal waveforms to devise a milling tool condition monitoring technique. Based on the Lipschitz exponent characteristics inferred from the vibration signals gathered by the integrated wireless vibration sensor tool holder system, a tool condition monitoring technique was developed. To connect with the varied tool wear states, a singularity analysis approach based on the wavelet transform was used. The most significant Lipschitz exponent features are discovered to be mean Lipschitz exponent values and quantity of singular points. According to the classification findings, the support vector machine learning technique was able to properly discern the tool wear condition with an accuracy of 86.1 percent.

2.2 Sounds as Methods in Tool Monitoring Systems

Shankar, Mohanraj, & Rajasekar, 2018 designed a tool monitoring system for keyway milling of 7075-T6 hybrid aluminium alloy composite with sound and machine force obtained during milling process. Using a microphone and milling tool dynamometer with NI USB 6221 DAQ card, sound pressure and machining force were captured throughout the milling operation and examined using LabVIEW. The ANFIS model and a MATLAB-based Neural Network were used to forecast the tool condition. When AI results surpass a value of 3, the condition gets dull and must be changed in order to continue the machining operation. This approach makes it easy to keep track of the machining process in a consistent manner. As compared to the ANFIS estimator, the feed-forward backpropagation neural network estimator gave the lowest mean square error.

K. feng Zhang, Yuan, & Nie, 2015 use acoustic emission and cutting sound as monitoring signals in a multi-sensor information fusion technique for tool condition monitoring (TCM). Each kind of signal was filtered, and features retrieved according to characteristics using time–frequency analysis methods and multi-fractal theories. The model of support vector machines (SVMs) ensemble utilised the decision level fusion approach to realise information fusion. For both categorization of tool wear state and prediction of tool wear amount, the combined decision outperforms the test that utilising only one type of signal, according to the test findings.

Shi, Wang, Chen, & Shao, 2015 developed a method based on empirical mode decomposition (EMD) and independent component analysis (ICA) to overcome the blind source separation problem of cutting sound signals in face milling is addressed, with the goal of isolating cutting directed sound signals from background sounds. The capacity of EMD to adaptively deconstruct an arbitrarily complex time series into a set of components termed intrinsic mode functions is one of its main advantages (IMFs). Experiments demonstrate that the suggested EMD-ICA approach can successfully separate cutting sound signals in face milling, with various source components associated to a normal and a damaged insert being retrieved. This allows for the identification of tool breakage.

Even though many researches have been conducted on effect of tool conditions on various process variables in the development of TCMs, these researches mainly focus on heavy machining where the machine is stationary and have proper fixture such as CNC machining, turning process, milling process, drilling process using milling machine etc. Thus, this study which focus on mobile, air drill is unprecedented, and a lot of works need to be done to explore its potentials.

CHAPTER 3

RESEARCH METHODOLOGY

3.1 Fabrication of Jig

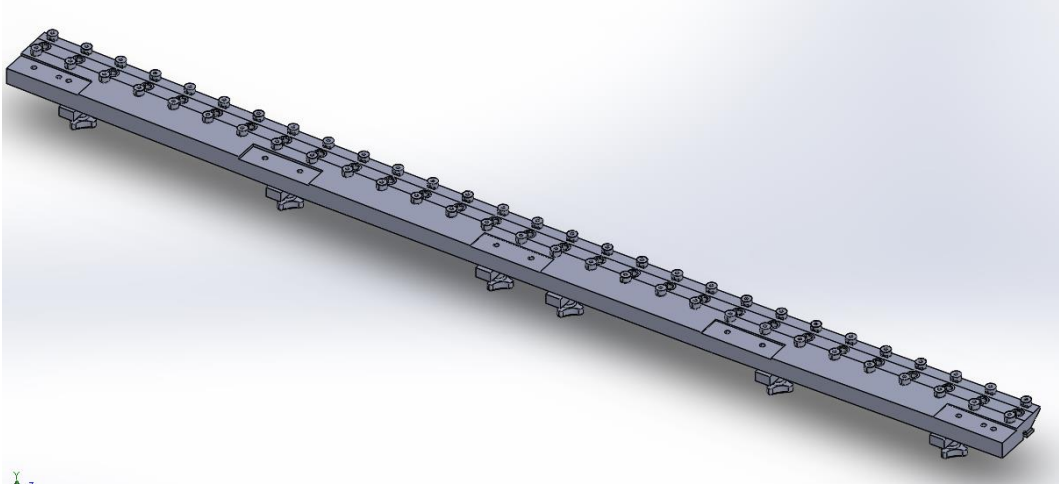


Figure 3-1: 3D model of jig used in industry for drilling of composite material

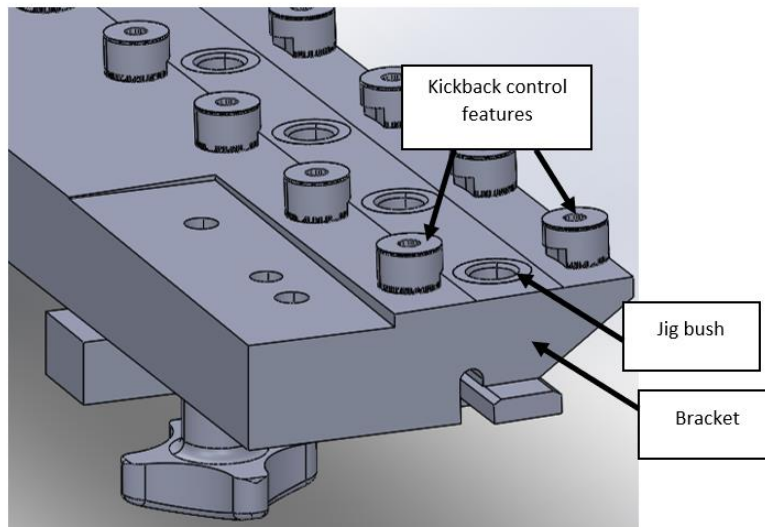


Figure 3-2: Closer look on features available on jig.

As can be seen in Figure 3-1 above, in the industry, the jig used to clamp the composite material consists of jig bush for drilling. The important features (such as Jig bush, kickback control features, bracket) and its respective dimensions were then taken as references for the designed jig which will be used for the experiment.

After multiple corrections and tests conducted, the finalized design of jig is as shown in Figure 3-3 below. The black colour parts which made up of all the intricate

features are printed with higher density than that of purple colour parts. In the experiment, the thin purple plate below will be clamped between the composite plates and the jaw of table clamp at one end and g clamp at the other end. This is to protect the composite plates from damages induced by clamping forces.



Figure 3-3: 3D printed jig

3.2 Preparation of CFRP Plates and GFRP Plates.

By using a hand cutter, CFRP plates and GFRP plates with areas of about 9mm×18.5mm as shown in Figure 3-4 below is cut from the scrap CFRP plates and GFRP plates obtained from the industry.



Figure 3-4: The CFRP plates (left) and the GFRP plates (right) with size of about 9cm×18.5cm.

3.3 Specification of LMS SCADAS Mobile, Accelerometer and Microphone.



Figure 3-5: LMS SCADAS Mobile

The data acquisitions systems used to collect vibration signals and sounds from accelerometers and microphone respectively was LMS SCADAS Mobile. Generally, LMS SCADAS Mobile hardware consists of ultralight yet robust systems of 2.5 kilograms (kg) that have a nominal 2.5- hour battery autonomy, to laptop-sized systems that can host from eight to 216 channels in a single frame.

Specifications of LMS SCADAS Mobile are as shown:

- Up to 204.8 kHz sampling rate per channel and throughput up to 14 MSamples/s

- 24-bit delta-sigma ADC technology
- 150-dB dynamic range
- Can include onboard CAN bus, dual tachometer and signal generator support
- Master-slave configurations for distributed systems and channel expansion
- High-speed Ethernet host interface
- Military-standard (MIL-STD)-810F qualified for shock and vibration
- Rugged design and low power consumption



Figure 3-6: Accelerometer

The model of accelerometer used was 3055B2T manufactured by Dytran Instrument, Inc. It has sensitivity of 100 mV/g, F.S. range of $\pm 50g$ for $\pm 5V$ output and can detect frequency in the range from 1-10k Hz. Full specifications of the accelerometer can be seen in Figure 3-7 below.

| SPECIFICATION | VALUE | | | UNITS |
|-------------------------------------|-------------------------------|----------------|----------------|----------|
| PHYSICAL | | | | |
| WEIGHT | 8.6 | | | grams |
| SIZE, HEX x HEIGHT | .50 x 0.62 | | | inches |
| MOUNTING PROVISION | 10-32 UNF-2B X .200 deep | | | |
| CONNECTOR, RADIALLY MOUNTED | 10-32 coaxial | | | |
| MATERIAL, BASE, CAP & CONNECTOR | titanium | | | |
| SEISMIC ELEMENT TYPE | ceramic, planar shear | | | |
| PERFORMANCE | | | | |
| | 3055B1T | 3055B2T | 3055B3T | |
| SENSITIVITY, ± 5% [1] | 10 | 100 | 500 | mV/g |
| RANGE F.S. FOR ± 5 VOLTS OUTPUT | ± 500 | ±50 | ±10 | g |
| FREQUENCY RANGE, ± 5% | 0.6 to 5000 | 1.0 to 5000 | 1.0 to 5000 | Hz |
| ± 10% | 1 to 10,000 | 1 to 10,000 | 1 to 10,000 | Hz |
| RESONANT FREQUENCY, NOM. | 32 | 32 | 32 | kHz |
| ELECTRICAL NOISE FLOOR (25Hz-25kHz) | 0.0002 | 0.00006 | 0.00005 | g rms |
| (1Hz-10kHz) | 0.0004 | 0.0001 | 0.0001 | g rms |
| LINEARITY [2] | ± 2 | ±2 | ±2 | % F.S. |
| TRANSVERSE SENSITIVITY, MAX. | 5 | 5 | 5 | % |
| ENVIRONMENTAL | | | | |
| | 3055B1T | 3055B2T | 3055B3T | |
| MAXIMUM VIBRATION/SHOCK | 600/5000 | 400/5000 | 200/5000 | ± g/g pk |
| TEMPERATURE RANGE, operational | -60 to +250 | -60 to +250 | -60 to +212 | °F |
| TEMPERATURE RANGE, TEDS operation | -40 to +185 | -40 to +185 | -40 to +185 | °F |
| SEAL, HERMETIC | Glass-to-metal and TIG welded | | | |
| COEFFICIENT OF THERMAL SENSITIVITY | .06 | .06 | .06 | %/°F |
| ELECTRICAL | | | | |
| | 3055B1T | 3055B2T | 3055B3T | |
| SUPPLY CURRENT [3] | 2 to 20 | 2 to 20 | 2 to 20 | mA |
| COMPLIANCE VOLTAGE | +18 to +30 | +18 to +30 | +18 to +30 | Vdc |
| OUTPUT IMPEDANCE, TYP. | 20 | 120 | 210 | Ω |
| BIAS VOLTAGE, +10.5 VOLTS NOM. | +11 to +13 | +11 to +13 | +11 to +13 | Vdc |
| DISCHARGE TIME CONSTANT, NOM. | 0.5 | 0.5 | 0.5 | sec |
| OUTPUT SIGNAL POLARITY | positive | | | |
| FOR ACCELERATION TOWARD TOP | | | | |
| ELECTRICAL ISOLATION, min | 10 | 10 | 10 | MΩ |
| CASE GROUND TO MOUNTING SURFACE | | | | |
| IEPE SENSOR WITH TEDS FEATURE | PER IEEE 1451.4 | | | |

Figure 3-7: Specifications of accelerometer



Figure 3-8: BSWA microphone

The model of microphone used was MA211 manufactured by BSWA technology. It is able to detect sound with frequency response in the range of 20 Hz to 100k Hz. The sound attenuation is less than 0.5dB. The full specification of the microphone is as shown in Figure 3-9 below:

| | |
|---|---|
| Models | MA211 |
| Diameter | 1/2 inch |
| Frequency Response (Ref: 250 Hz, ±0.2 dB) | 20 Hz ~ 100 kHz |
| Attenuation (10 Hz ~ 100 kHz) | < 0.5 dB |
| Input Impedance | > 5 GΩ |
| Output Impedance | < 110 Ω |
| Electrical Noise | A-weighting < 2.0 μV 20 Hz ~ 20 kHz < 6.0 μV |
| Max Output Voltage | 3.5 Vrms |
| Power Requirement | ICP (2 ~ 20 mA) |
| Operating Temperature | -20°C ~ 80°C |
| Operating Humidity | 0 ~ 98% RH |
| Length | 71 mm |
| Output Connector | BNC |
| Thread for Microphone | Φ11.7 mm x 60 UNS |

Figure 3-9: Full specification of the microphones

3.4 Setup of LMS SCADAS Mobile, Accelerometer and Microphone

3 accelerometers with different code name are placed at location near the spindle of air drill, middle body of the drill and near the handle of the drill as shown in Figure 3-10 below. During the selection of the locations on air drills, a few factors on the surface of locations are taken into considerations such as the surface need to be metallic to reduce damping effect, the surface of part need to be non-moving parts and the surface cannot overlap with the hand holding region.

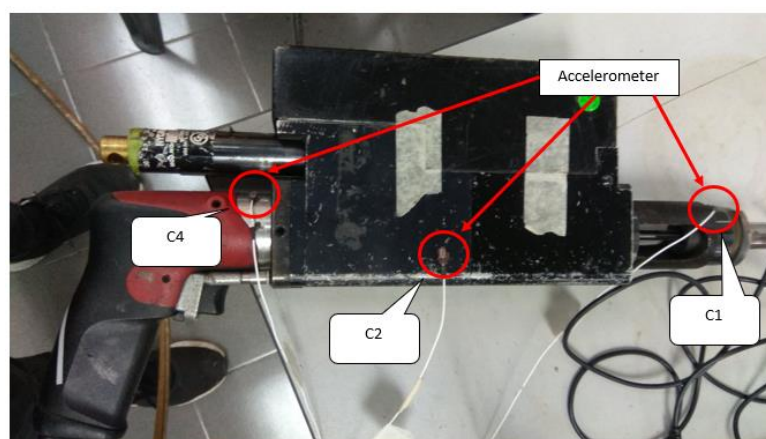


Figure 3-10: Positions of accelerometer C1, C2 and C4 on air drills

Microphone is placed on a stand located at distance 1 meter away from the air drill when the drilling occurred. The setups of overall systems can be summarized in schematic diagram as shown in Figure 3-11 below:

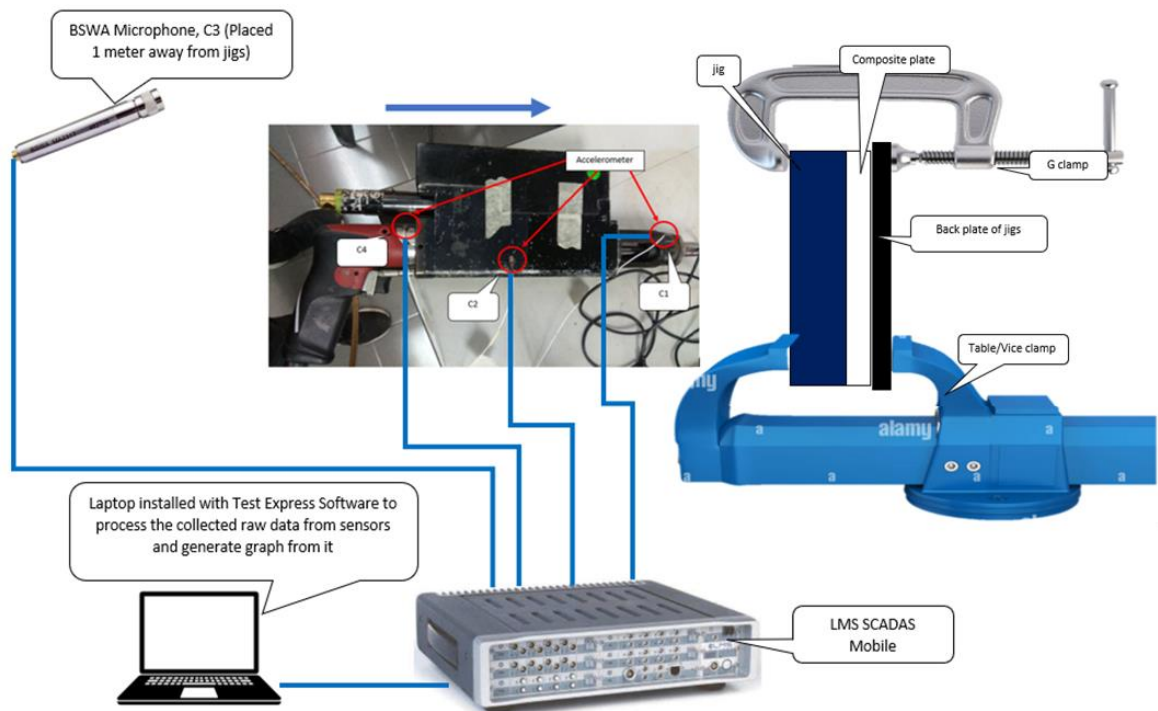


Figure 3-11: Schematic Diagrams of the experiment setups.

3.5 Preparation of Drill Bits

3 drill bits are obtained from Spirit AeroSystems Sdn Bhd where 1 of it is sharp one while another 2 of it is blunt one (discarded drill bit after been used for many times). To make a chipped off drill bit, metal file is used to file on the cutting edge of blunt drill bit until chipped off have been observed on multiple sites of the cutting edge. Each drill bit will be used to drill 3 holes on CFRP plates and GFRP plates respectively.

3.6 Conduction of the Experiment

The pressure of compressed air available in SME Lab is about 7 bar. The air tubing with adapter on it is used to connect the tap for compressed air to air drill. For each type of plates and each type of drill bit, 3 holes will be drilled. And for each drilling attempt, the vibration of the air drill and the noise produced will be measured and recorded. After a hole is drilled, it will be covered with a masking tape marked with codes according to Table 3-1 below.

Table 3-1: Codes assigned for each hole

| Drill Bit condition | CFRP | | | GFRP | | |
|---------------------|------|-----|-----|------|-----|-----|
| | 1 | 2 | 3 | 1 | 2 | 3 |
| Sharp | S1 | S2 | S3 | S4 | S5 | S6 |
| Blunt | B1 | B2 | B3 | B4 | B5 | B6 |
| No Drill Bit | N1 | N2 | N3 | - | | |
| Chipped Off | CH1 | CH2 | CH3 | CH4 | CH5 | CH6 |



Figure 3-12: The posture and handling of the air drill during drilling of composite plate.

CHAPTER 4

RESULT AND DISCUSSION

In this experiment, 3 types of data are obtained which are amplitude versus time graph, FFT graph and Alicona images. Table 5-1 until Table 5-6 show vibrations amplitude versus time graph obtained from accelerometer C1, C2 and C4 during drilling of the CFRP plate and GFRP plate. Table 5-7 and Table 5-8 shows sound amplitude versus time graph obtained from microphone C3 during drilling of CFRP plate and GFRP plate.

On the other hand, Table 4-1 to Table 4-6 show FFT graph obtained from vibration measured using accelerometer C1, C2 and C4 during drilling of CFRP plate and GFRP plate. Table 4-7 and Table 4-8 show FFT graph measured from microphone C3 during drilling of CFRP plate and GFRP plate. Meanwhile, Table 4-11 and Table 4-12 shows images of drilled holes on of front side and back side of CFRP plate respectively. Table 4-13 and Table 4-14 shows images of drilled holes on of front side and back side of GFRP plate respectively.

4.1 Amplitude versus Time Graph

From Table 5-1 until Table 5-6, no noticeable pattern on shape of the amplitude versus time graph that can be used to correlate it with condition of drill bit. Besides, properties of vibration signal such as average amplitude and RMS of the spectrum of vibration obtained from amplitude versus time graph cannot be correlated to different conditions of drill bits. As can be seen from the graph obtained from drilling of CFRP plate using chipped off drill bit, it shows that the time when measurement of vibration and sound starts are different, it is usually earlier than the time drilling of the plate commence but the timing when the measurement start is not constant from one to another measurement. These show that properties of the signal such as average amplitude and RMS of overall vibration spectrum obtained from this amplitude versus time graph are not reliable enough in TCM to predict the condition of the drill bit unless the TCM system can start the measurement on the instant the drill switch is pressed.

However, there are still other property of vibration signals which response accordingly to condition of drill bits. From Figure 4-1, there was a trend of increasing

maximum amplitude or also known as peak amplitude of vibration with condition of drill bit arranged in order: sharp, no drill bit, blunt and chipped off. This pattern is observed on vibration signals of air drill measured by accelerometer C1 from attempt 2, attempt 3 and average of all 3 attempt of drilling on CFRP plate. On the other hand, from Figure 4-2, increasing trend have also been observed but with condition of drill bit arranged in order: no drill bit, blunt, chipped off and sharp. Similar to pattern in Figure 4-1, this pattern is also observed on vibration signals of air drill measured by accelerometer C1 from attempt 2, attempt 3 and average of all 3 attempt of drilling on GFRP plate. Difference in the order of drill bit condition to produce similar trend proved that type of composite plate have significant effect on vibrations signal produced by different conditions of drill bit. Drilling attempt 1 did not produce similar trend as other drilling attempts on same plate most likely due to difference in strength of grips exerted by air drill user. Vibrational energy absorption by human hand increase with strength of user gripping force(Burström, 1994).

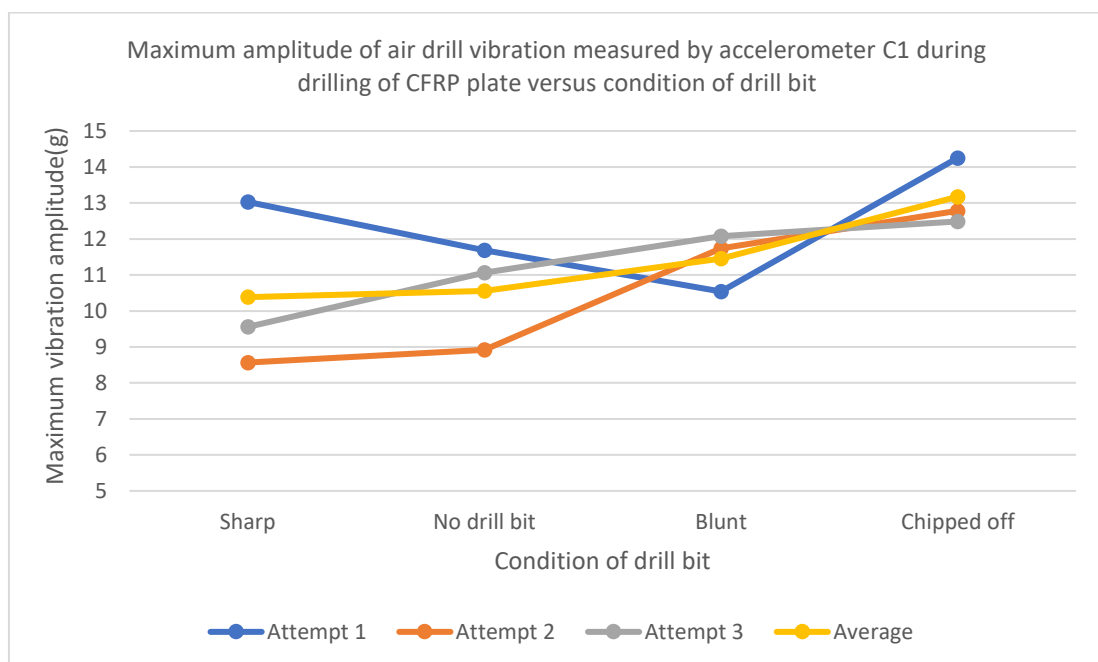


Figure 4-1: Maximum amplitude of air drill vibration measured by accelerometer C1 during drilling of CFRP plate versus condition of drill bit

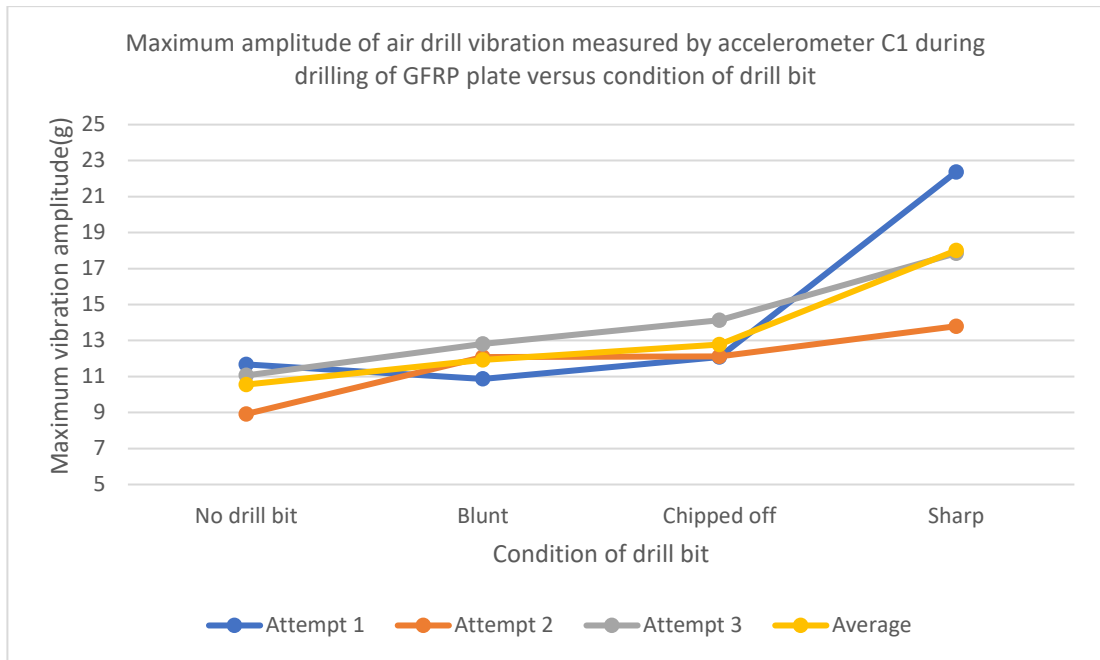


Figure 4-2: Maximum amplitude of air drill vibration measured by accelerometer C1 during drilling of GFRP plate versus condition of drill bit

Even though trend of maximum amplitude is observed from vibration measured by accelerometer C1 during drilling of both type of composite plate, such trend cannot be observed from vibration signals obtained from accelerometer C2 during drilling of CFRP plate. There are no more than 2 graph line in Figure 4-3 that shows similar patterns. This can be attributed to longer distance of accelerometer C2 from drill bit and inconsistent grip force exerted by user. However, there are present of trend from vibration signals obtained from accelerometer C2 during drilling of GFRP plate. From Figure 4-4, drilling attempt 1, attempt 2 and average of all 3 attempts showing pattern of increasing peak amplitude when conditions of drill bit is arranged in order: no drill bit, chipped off, blunt and sharp. Trend can be observed in drilling of GFRP plate, but no CFRP plate further prove the effect of type of composite plate on vibration signal produced by different conditions of drill bit.

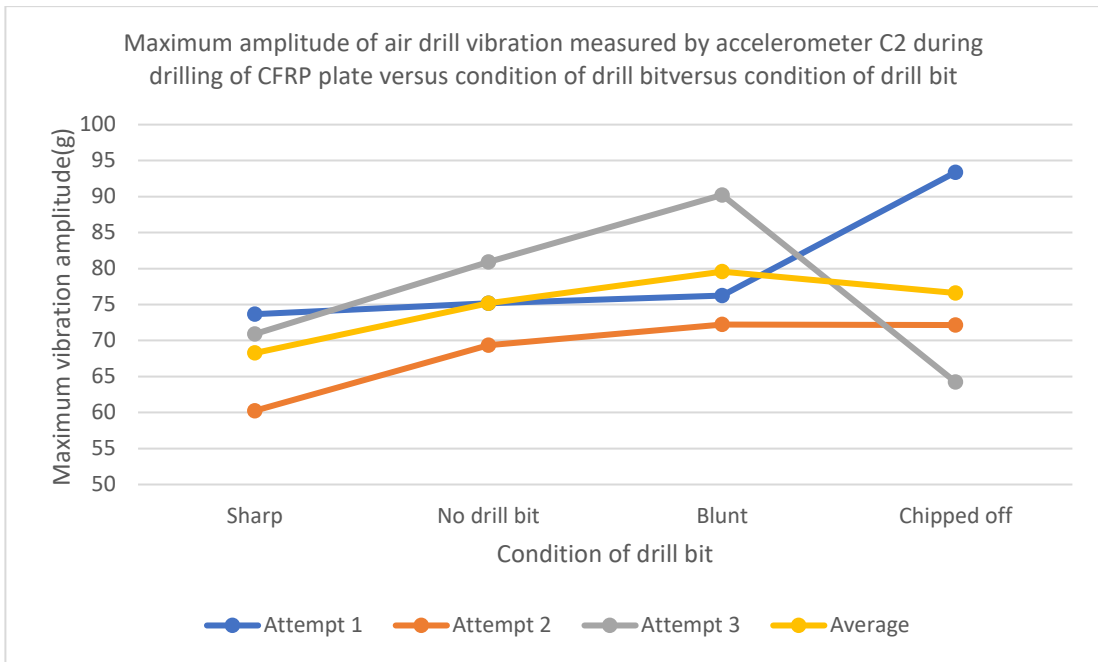


Figure 4-3: Maximum amplitude of air drill vibration measured by accelerometer C2 during drilling of CFRP plate versus condition of drill bit

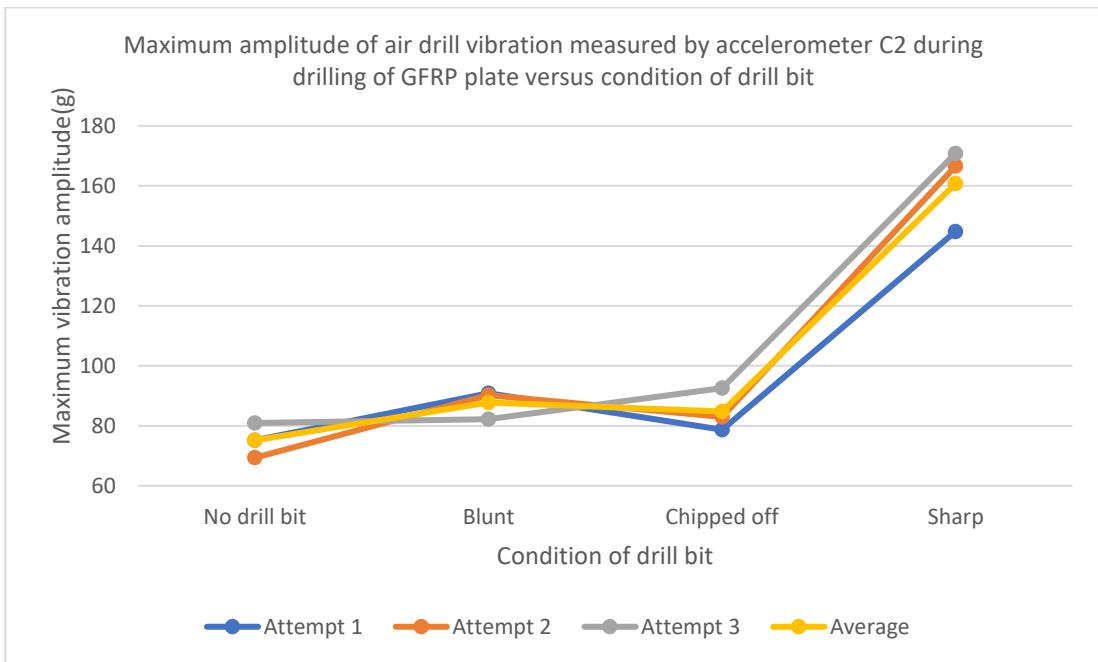


Figure 4-4: Maximum amplitude of air drill vibration measured by accelerometer C2 during drilling of GFRP plate versus condition of drill bit

For vibration signal collected by accelerometer C4, there are no trends of maximum amplitude of vibrations observed during drilling of either CFRP plate or GFRP plate. From Figure 4-5, all 4 graphs lines showing different pattern respectively. From Figure 4-6, even though more than 2 graph lines seems to have similar pattern

on first glance, only attempt 2 and average peak amplitude of all 3 attempts exhibit similar pattern. Without considering average peak amplitude of all 3 attempts, 3 drilling attempts did not exhibit similar trend. The absent of trend of maximum amplitude from vibration signal measured by accelerometer C4 is due to its long distance from the drill bit. The vibrations have interrupted by vibrations absorption by grips at the middle of air drill and grips at the handle of air drill before it is measured by accelerometer C4.

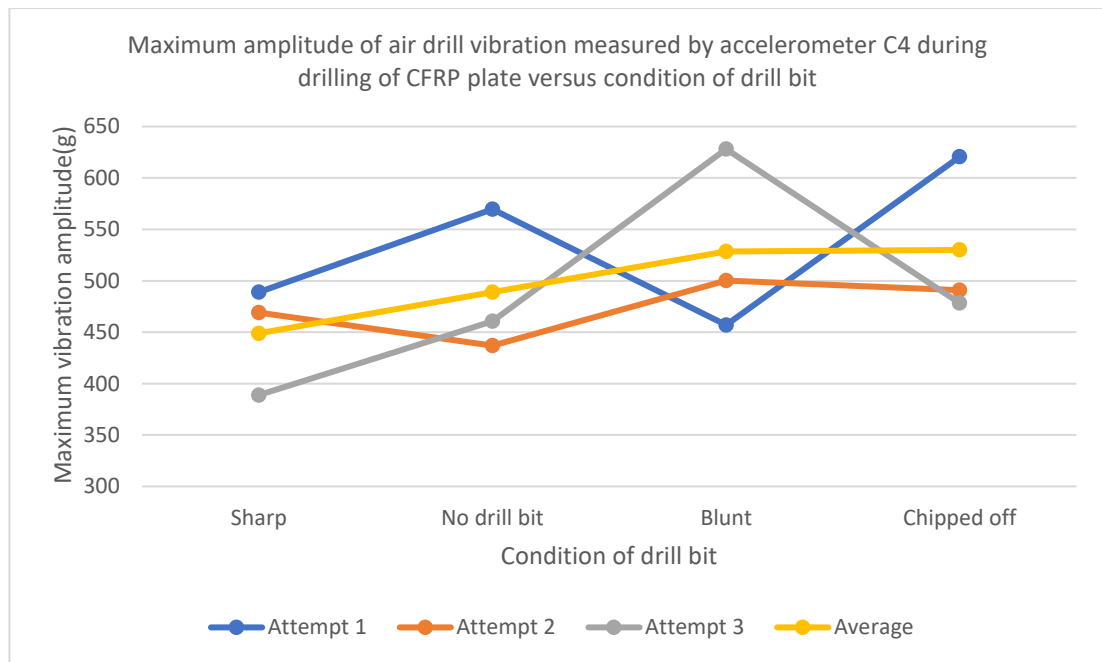


Figure 4-5: Maximum amplitude of air drill vibration measured by accelerometer C4 during drilling of CFRP plate versus condition of drill bit

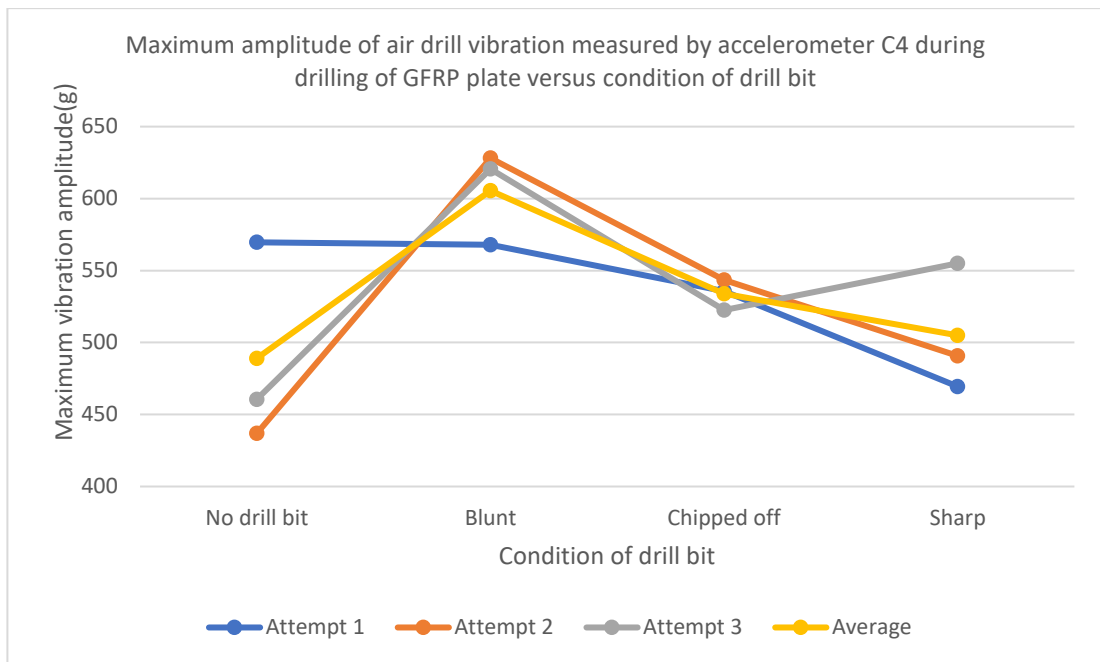


Figure 4-6: Maximum amplitude of air drill vibration measured by accelerometer C4 during drilling of GFRP plate versus condition of drill bit

From Table 5-7, Table 5-8, Figure 4-7 and Figure 4-8, sound does not provide notable information or patterns that can correlate to conditions of drill bit. From Figure 4-7 and Figure 4-8, all 3 drilling attempts exhibit different maximum amplitude pattern from each other. The reason the sound produced during of composite plate seems to be irrelevant to condition of drill bit was mostly likely due to present of significant background noise. This reason is supported by other researchers, stating that the main problem with using sound monitoring to capture sensory data is that the signal-to-noise ratio of usable data about tool wear is relatively low (Battista, Knapp, McGee, & Goebel, 2007; Sick, 2002).